Journal of Organometallic Chemistry 880 (2019) 124–133

Contents lists available at ScienceDirect

Journal of Organometallic Chemistry

journal homepage: www.elsevier.com/locate/jorganchem

Synthesis and properties of stimuli-responsive ferrocene-and azobenzene-based copolymers P(FHEMA-*co*-MAAT)s

Amin Khan, Li Wang*, Haojie Yu**, Muhammad Haroon, Raja Summe Ullah, Ahsan Nazir, Tarig Elshaarani, Muhammad Usman, Shah Fahad, Kaleem-ur-Rehman Naveed

State Key Laboratory of Chemical Engineering, College of Chemical and Biological Engineering, Zhejiang University, Hangzhou, 310027, PR China

ARTICLE INFO

Article history:
Received 16 September 2018
Received in revised form
24 October 2018
Accepted 31 October 2018
Available online 3 November 2018

Keywords:
Redox responsive
Photo responsive
Organometallic

ABSTRACT

Three novel polymers (P(FHEMA-*co*-MAAT)s) having redox and photoresponsive moieties were prepared by free radical polymerization. The structures and molecular weights of the synthesized copolymers were characterized by nuclear magnetic resonance (^{1}H NMR) and gel permeation chromatography (GPC) respectively. Thermal properties, optical features and electroactive properties were studied with the help of thermogravimetric (TG), differential thermogravimetric (DTG) analysis, ultraviolet-visible spectroscopy (UV-vis) and cyclic voltammetry (CV). It was seen that synthesized copolymers had excellent redox and photoresponsive properties. These results exhibited that these polymers can be applied further for redox/photo responsive information storage devices.

1. Introduction

Organometallic complexes containing photoresponsive group are of great interest for the world as these complexes can provide dual stimuli effect [1]. Among available organometallic systems, ferrocene-based polymers can provide many exciting applications due to the unusual properties of ferrocene moiety [2]. Ferrocene has many unique features such as good thermal stability, 3D structure, high redox activity and easy solution processability [3,4]. A redox process of ferrocene can alter the properties of the polymeric material. Thus, depending on their redox state (oxidized or reduced) the polymer usually presents different chemical, electronic, optical or mechanical properties. These attributes have initiated a new era of polymers containing ferrocene component [5,6]. On the other hand, photoresponsive chromophores have also got importance in the past few decades [7,8]. Among photoresponsive moieties, azobenzene-based moieties have received considerable attention due to their several properties such as rapidly reversible photoisomerization, low flammability, bright color and good stability [9–11]. Azobenzene shows two significant isomerization trends depending on the type of external exposure. The first trend originates due to the ultraviolet irradiation which causes *trans* to *cis* isomerization. This isomerization brings a decrease in absorption intensity at 330–380 nm (π-π^* transition) and an increase in absorption intensity at 420–450 nm (n-π^* transition). The second substantial trend can be observed due to the visible light or heat which causes *cis* to *trans* isomerization [12]. These photo conformational changes in azobenzene can change its dipole moment, absorption capacity and geometry [13]. The communication of electronic states can be manipulated by interlinking ferrocene and azobenzene group with a π-conjugated system or an organic linker with suitable length [14]. Nishihara and coworkers were among the pioneers who reported the unique properties of ferrocene-based azobenzenes in which the one-electron oxidation of the compound decreased the thermodynamic stability of the *cis*-azobenzene group bonded to ferrocene [15]. This oxidation provided a corridor towards a *trans* rich mixture in the Fe^{3+} state using monochromatic green light and a *cis*-rich mixture due to the electrochemically reduced state of ferrocene (Fe^{2+}). This electro-photo probe-based system proved as a good on-off switching model. Alternatively, different kinds of functional groups can alter the *cis-trans* isomerization of organic azobenzene as well [16,17]. Thus, the photoisomerization behavior of azobenzene can be changed by the introduction of the appropriate functional group. It is expected that introducing a methyl group on the electron-rich benzene rings of azobenzene can decrease the photo-oxidation, photoinduced side reactions and $\pi-\pi$ stacking of chromophores [18,19]. What is noteworthy is that, on a

* Corresponding author.
** Corresponding author.
E-mail addresses: opl_wl@dial.zju.edu.cn (L. Wang), hjyu@zju.edu.cn (H. Yu).

https://doi.org/10.1016/j.jorganchem.2018.10.033
0022-328X/

combination of ferrocene and azobenzene in one system, the ferrocenyl center affects the isomerization of azobenzene by intramolecular interactions [20]. By taking this all idea into the account, different ferrocene-and azobenzene-based copolymers (P(FHEMA-*co*-MAAT)s) have been synthesized and their reversible electro/photo responsive properties have been analyzed in this work.

2. Experimental section

2.1. Materials

Tetrahydrofuran (THF, analytical reagent (AR)), dichloromethane (DCM, AR), methanol (AR), pyridine (AR) and triethylamine (Et_3N, AR) were purchased from Sinopharm Chemical Reagent Co., Ltd. Ferrocene carboxylic acid (AR) was purchased from Aladdin. Hydroxyethyl methacrylate (HEMA, 96%) and methacrolyl chloride (95%) were provided by Acros Organics. O-aminoazotoluene (97%) was purchased from Tokyo Chemical Industry (TCI) Co., Ltd. Tetrabutylammonium tetrafluoroborate (Bu_4NBF_4) and azobisisobutyronitrile (AIBN) were supplied by J& K Scientific Co. Ltd. Activated 4A-type molecular sieves were used to dry the pyridine. DCM, THF and Et_3N were firstly dried by activated 4A-type molecular sieves. After that, DCM and Et_3N were distilled over calcium hydride while THF was distilled over potassium. Other chemicals were used without further purification.

2.2. Synthesis of ferrocene carbonyl chloride

Ferrocenecarbonyl chloride was prepared in a schlenk line system to ensure moisture free environment as reported before [21]. In a typical reaction, ferrocene carboxylic acid (10.3601 g, 45.0 mmol) was firstly dried under vacuum at 50 °C for 30 min and then dissolved in 75.0 mL of freshly distilled DCM. After that, pyridine (7.20 mL, 90.36 mmol) was added to the previous solution followed by the dropwise addition of oxalyl chloride (7.75 mL, 90.36 mmol) at 25 °C. The reaction mixture was stirred for 30 min first at 25 °C and then refluxed for 5 h. The contents of the reaction flask were evaporated under vacuum and petroleum ether (80.0 mL) was added. The mixture was stirred for 2 h at 90 °C at this stage. At last, the solvent was evaporated to get the dried ferrocene monocarbonyl chloride.

2.3. Synthesis of 2-(methacryloyloxy)ethyl ferrocene carboxylate (FHEMA)

FHEMA was prepared as reported before [22]. To obtain FHEMA, ferrocene monocarbonyl chloride (6.1400 g, 24.6 mmol) was firstly dissolved in 60.0 mL of THF. Afterward, pyridine (1.93 mL, 24.6 mmol) and HEMA (3.01 mL, 24.7 mmol) were added to the previous solution under Ar atmosphere. This reaction mixture was refluxed for 5 h. After completing the reflux, the precipitates were removed from the reaction mixture by filtration. After that, the obtained filtrate was evaporated on a rotary evaporator. This crude product was washed successively by a saturated solution of Na_2CO_3 (250 mL × 3) and deionized water (250 mL × 3) to obtain the final pure product. This product was placed in a vacuum oven at 40 °C to get FHEMA.

2.4. Synthesis of methacrylo-2-aminoazotoluene (MAAT)

MAAT was prepared according to the reported procedure [23]. In a typical reaction, o-aminoazotoluene (AAT) (4.6011 g, 20.4 mmol) was firstly dried under vacuum for 30 min at room temperature and then dissolved in 80.0 mL of DCM. After that, triethylamine (3.00 mL, 21.5 mmol) was added in the same reaction flask at the room temperature followed by the dropwise addition of methacrolyl chloride (2.50 mL, 25.5 mmol) at 0 °C. The reaction was carried out for 2 h at this stage and then for 8 h at room temperature. Afterward, the precipitates were removed from the reaction mixture by filtration. This crude product was washed successively by a saturated solution of Na_2CO_3 (250 mL × 3) and distilled water (250 mL × 3) to obtain the final pure product. This product was placed in a vacuum oven at 40 °C to get reddish yellow MAAT.

2.5. Synthesis of poly 2-(methacryloyloxy) ethyl ferrocene carboxylate (PFHEMA)

For obtaining poly 2-(methacryloyloxy) ethyl ferrocene carboxylate, free radical polymerization was carried out [24]. In a typical synthesis, FHEMA (500.3 mg, 1.75 mmol) and AIBN (2.9 mg, 0.0176 mmol) were dissolved in DMF (2.0 mL). The flask was purged with Ar gas first for 15 min and then the reaction was left for 12 h at 80 °C. The reaction mixture was precipitated in 250 mL of methanol to remove the unreacted monomers. After that, the solvent with precipitates was centrifuged. The obtained residual solid was dissolved in THF and precipitated again in 250 mL of methanol. The final polymer was obtained with centrifugation and dried in a vacuum oven for the complete removal of residual solvents.

2.6. Synthesis of poly (methacrylo-2-aminoazotoluene) (PMAAT)

For obtaining poly (methacrylo-2-aminoazotoluene), free radical polymerization was used [24]. In a typical synthesis, MAAT (306.1 mg, 1.04 mmol) and AIBN (1.4 mg, 0.0085 mmol) were dissolved in DMF (2.0 mL). The flask was purged with Ar gas first for 15 min and then the reaction was left for 12 h at 80 °C. The reaction mixture was precipitated in 250 mL of methanol to remove the unreacted monomers. After that, the solvent with precipitates was centrifuged. The obtained residual solid was dissolved in THF and precipitated again in 250 mL of methanol. The final polymer was obtained with centrifugation and dried in a vacuum oven for the complete removal of residual solvents.

2.7. Synthesis of poly (2-(methacryloyloxy) ethyl ferrocene carboxylate-co-(methacrylo aminoazo toluene) P(FHEMA-co-MAAT)

For the typical copolymerization of FHEMA and MAAT, free radical polymerization technique was adapted [19]. The synthetic procedure for all the obtained polymers is same with the difference in the mole ratios of monomers (FHEMA, MAAT). Therefore, the synthesis of P(FHEMA-*co*-MAAT)-1 was taken as an example. In the typical synthesis, FHEMA (0.3401 g, 0.99 mmol), MAAT (0.2801 g, 0.97 mmol) and AIBN (0.0038 g, 0.02 mmol) were dissolved in DMF (2.0 mL). The flask was then purged with Ar gas for 0.5 h to remove any dissolved oxygen. The reaction was carried out for 12 h at 80 °C. The reaction mixture was precipitated in 250 mL of methanol to remove any unreacted monomers. After that, the solvent with precipitates was centrifuged. The obtained residual solid was dissolved in THF and precipitated again in 250 mL of methanol. Finally, the precipitates were centrifuged, filtered and dried in a vacuum oven to obtain a yellowish solid.

2.8. Characterization

The ^1H NMR spectra of the synthesized copolymers were measured using a Bruker Advanx-600 MHz NMR spectrometer. Gel permeation chromatography (GPC) analysis was carried out with waters 1524/2414 as GPC instrument and THF as the mobile phase. All the copolymers were calibrated against

polymethylmethacrylate (PMMA). Thermogravimetric analysis (TGA) was performed with a heating rate of 10 °C/min using TA-Q500 (Metler-Toledo). Differential scanning calorimetry (DSC) was executed with a heating rate of 10 °C/min using Perking Elmer (PE) DSC 7. UV-vis spectra of the samples were measured using the Unico spectrophotometer. The concentration of the solution was 0.05 mM. The CV analysis was measured with a CHI-630A electrochemical analyzer (CH Instruments, Inc., Austin, Texas). For all the samples, the concentration of polymers and electrolyte (Bu_4NBF_4) was 0.5 mM and 0.1 M respectively. A platinum wire electrode was used as the counter electrode and silver (Ag) electrode as a reference electrode. The glassy carbon working electrode was given a mirror finish using 0.05 μm Al_2O_3 paste followed by washing under ultrasonication with alcohol/deionized water for 30 s and finally dried at room temperature prior to use.

3. Results and discussions

3.1. Synthesis and characterization of FHEMA

Esterification reaction between ferrocene carbonyl chloride and HEMA was carried out to synthesize FHEMA (Scheme 1a). The structure of FHEMA was confirmed by ^{1}H NMR (Fig. 1a). The data of chemical shifts for FHEMA was as follows: δ (ppm) = 6.07 (1H, H_a), 5.71 (1H, H_b), 4.71 (2H, H_c), 4.46 (2H, H_d), 4.38 (4H, H_e, H_f), 4.18 (5H, H_g), 1.88 (3H, H_h).

3.2. Synthesis and characterization of MAAT

The synthesis of MAAT was successfully performed by amidation reaction of o-aminoazotoluene and methacrolyl chloride (Scheme 1b). The structure of MAAT was elucidated by ^{1}H NMR (Fig. 1b). Following chemical shifts were obtained in a result: δ (ppm) = 9.44 (1H, H_a), 7.29–7.77 (7H, H_b-H_h) 5.89 (1H, H_i), 5.54 (1H, H_j), 2.66 (3H, H_k), 2.31 (3H, H_l), 1.98 (3H, H_m).

3.3. Synthesis and characterization of PFHEMA, PMAAT and P(FHEMA-co-MAAT)s

Free radical polymerization was executed to synthesize PFHEMA, PMAAT and P(FHEMA-*co*-MAAT)s. Homo-polymerization and copolymerization of FHEMA and MAAT were performed using AIBN as a free radical initiator. The synthetic routes of

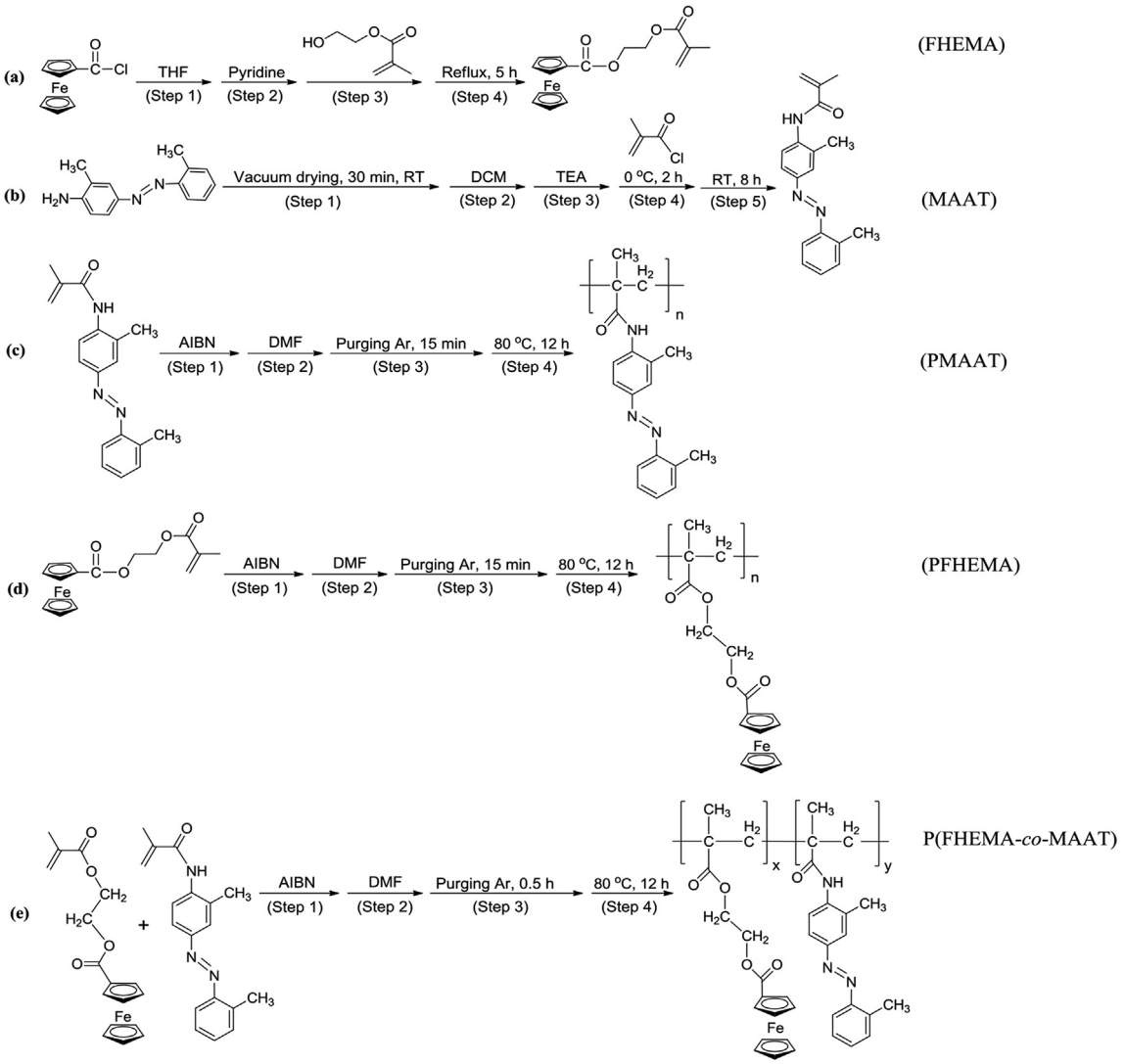

Scheme 1. Synthetic reactions for (a) FHEMA, (b) MAAT, (c) PMAAT, (d) PFHEMA and (e) P(FHEMA-*co*-MAAT).

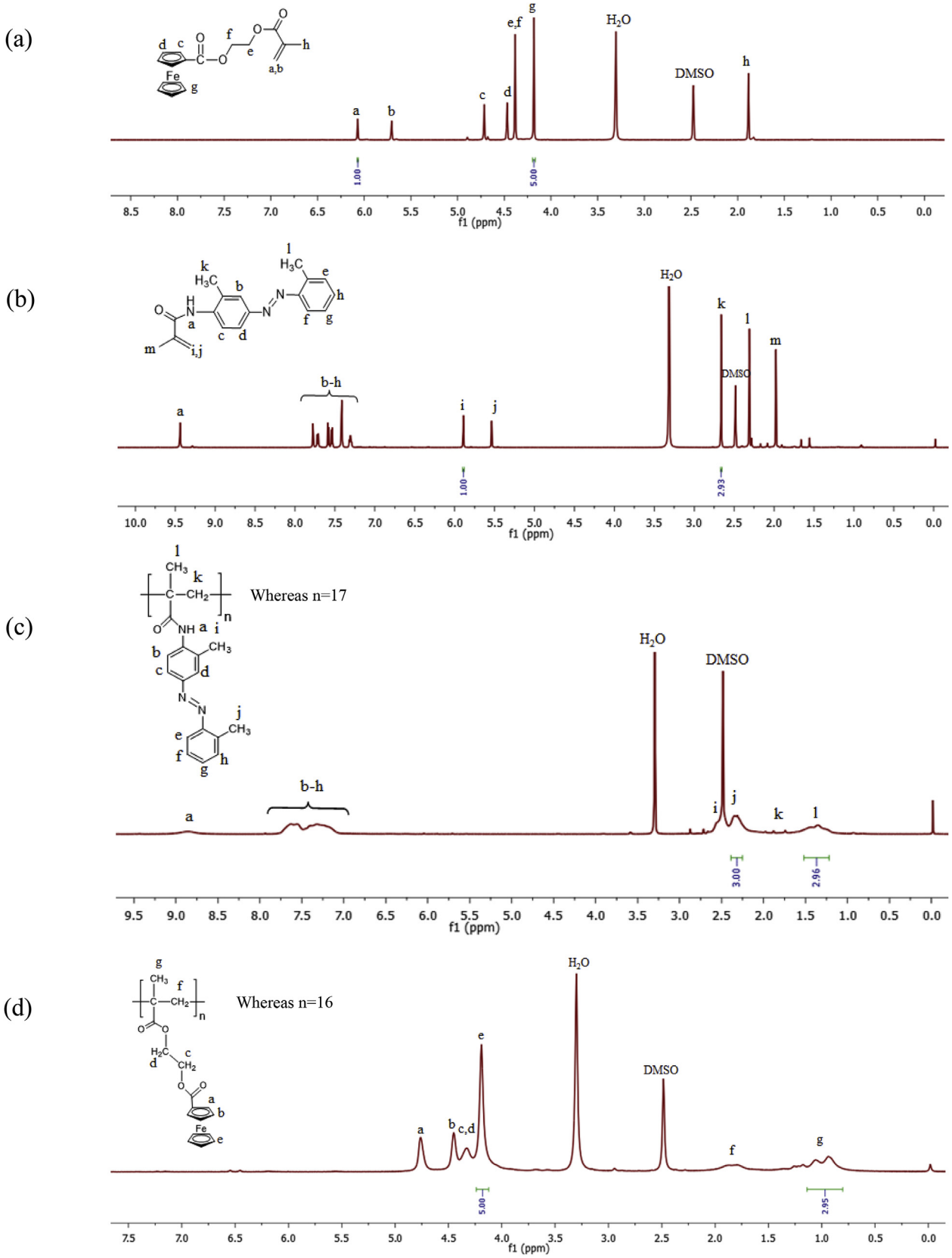

Fig. 1. [1]HNMR spectra of (a) FHEMA, (b) MAAT, (c) PMAAT and (d) PFHEMA.

homopolymers and copolymers have been given in Scheme 1(c-e). Different mole ratios of monomers were taken to synthesize different copolymers. The characteristic peaks of the synthesized homopolymers and copolymers were confirmed by ^{1}H NMR spectra as shown in Fig. 1(c and d) and Fig. 2 respectively.

The characteristic peak shifts for PFHEMA were as follows: δ (ppm) = 4.76 (2H, H_a), 4.45 (2H, H_b), 4.33 (4H, H_c, H_d), 4.19 (5H, H_e), 1.66–2.01 (2H, H_f), 0.84–1.15 (3H, H_g). The characteristic peak shifts for PMAAT were as follows: δ (ppm) = 8.86 (1H, H_a), 7.13–7.72 (7H, H_b-H_h) 2.50–2.61 (3H, H_i), 2.24–2.38 (3H, H_j), 1.71–1.98 (2H, H_k), 1.22–1.51 (3H, H_l).

The chemical shifts for P(FHEMA-*co*-MAAT)-1 were as follows: δ (ppm) = 8.86 (1H, H_a), 7.16–7.77 (7H, H_b-H_h) 4.72 (2H, H_i), 4.35 (6H, H_j, H_k, H_l), 4.15 (5H, H_m), 2.60 (3H, H_n), 2.37 (3H, H_o), 1.77–2.08 (4H, H_p, H_q), 0.91–1.28 (6H, H_r, H_s).

The chemical shifts for P(FHEMA-*co*-MAAT)-2 were as follows: δ (ppm) = 8.84 (1H, H_a), 7.21–7.78 (7H, H_b-H_h) 4.74 (4H, H_i), 4.39 (12H, H_j, H_k, H_l), 4.16 (10H, H_m), 2.62 (3H, H_n), 2.37 (3H, H_o), 1.72–2.08 (6H, H_p, H_q), 0.86–1.23 (9H, H_r, H_s).

The chemical shifts for P(FHEMA-*co*-MAAT)-3 were as follows: δ (ppm) = 8.83 (1H, H_a), 7.24–7.77 (7H, H_b-H_h) 4.75 (6H, H_i), 4.42 (18H, H_j, H_k, H_l), 4.17 (15H, H_m), 2.66 (3H, H_n), 2.37 (3H, H_o), 1.64–2.10 (8H, H_p, H_q), 0.81–1.28 (12H, H_r, H_s).

The synthetic details of the copolymers (P(FHEMA-*co*-MAAT)s) are mentioned in Table 1 whereas Table 2 shows the details of molecular weights and mole ratios of copolymers.

Fig. 2 represents the comparison of ^{1}H NMR spectra of P(FHEMA-*co*-MAAT) copolymer. The results indicated that the peak area between 6.75 and 8.0 ppm belong to azobenzene, while the signals between 4.0 and 5.0 ppm belong to ferrocene. The disappearance of a double bond having a chemical shift between 5.5 and 6.5 ppm indicated that the unreacted monomers were completely removed from the polymers. Fig. 3A shows the GPC curves of the different synthesized polymers and it can be seen that the sample P(FHEMA-*co*-MAAT)-2 and P(FHEMA-MAAT)-3 did not show a mono distinct peak in comparison with P(FHEMA-*co*-MAAT)-1. This might be due to the uncontrolled polymerization route. Fig. 3B and C shows the thermal analysis (TGA and DTG) and Fig. 3D explains

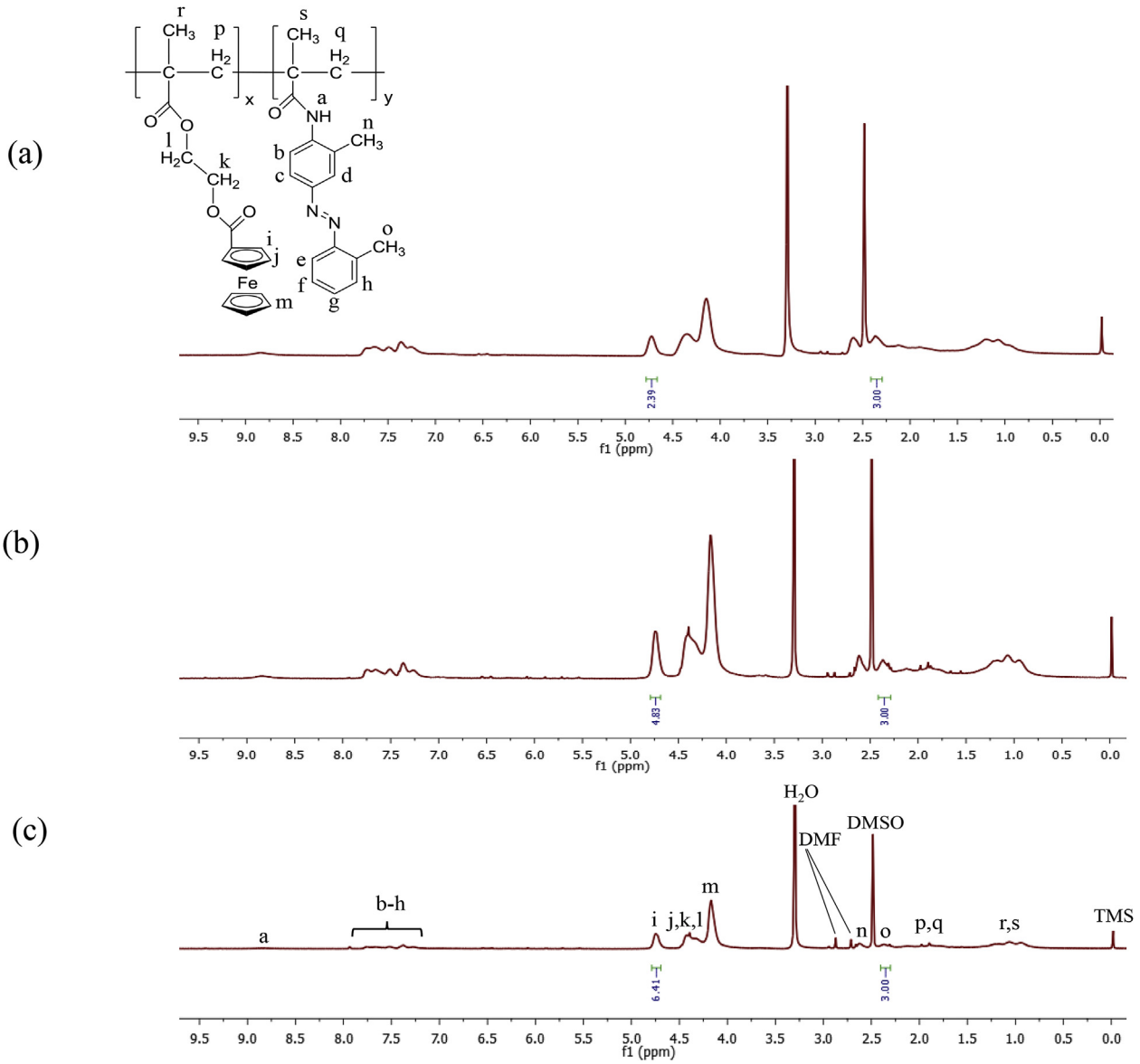

Fig. 2. ^{1}HNMR spectra of (a) P(FHEMA-*co*-MAAT)-1, (b) P(FHEMA-*co*-MAAT)-2 and (c) P(FHEMA-*co*-MAAT)-3.

Table 1
Synthetic details of P(FHEMA-*co*-MAAT)s.

Sample	Step 1							Step 2	Step 3	Step 4	
	FHEMA (A)		MAAT (B)		AIBN		Mole ratio	DMF	Ar purging	T	t
	g	mmol	g	mmol	g	mmol	A:B	mL	h	°C	h
P(FHEMA-*co*-MAAT)-1	0.3401	0.99	0.2801	0.97	0.0038	0.02	1:1	2.0	0.5	80	12
P(FHEMA-*co*-MAAT)-2	0.6801	1.98	0.2915	1.01	0.0049	0.03	2:1	2.0	0.5	80	12
P(FHEMA-*co*-MAAT)-3	1.0211	2.98	0.2811	0.98	0.0065	0.04	3:1	2.5	0.5	80	12

Table 2
GPC results and ratios of each unit.

Sample	P(FHEMA-*co*-MAAT)s[a]			P(FHEMA-*co*-MAAT)s[c]		
	Mn	Mw	PDI	(x:y)[b]	m(FHEMA)	n(MAAT)
P(FHEMA-*co*-MAAT)-1	4970	7983	1.60	1.19:1	4	3
P(FHEMA-*co*-MAAT)-2	8277	15472	1.86	2.41:1	8	3
P(FHEMA-*co*-MAAT)-3	7887	14946	1.89	3.20:1	9	2

[a] Determined by GPC data.
[b] Determined by ^{1}H NMR results whereas x and y are the number of mole ratios attached with FHEMA and MAAT respectively and.
[c] Calculated with the help of GPC and ^{1}H NMR results whereas m and n are the number of repeating units for FHEMA and MAAT respectively.

the differential scanning calorimetry (DSC) of the synthesized polymers. Fig. 3B explains the multistage degradation process of the polymers. The initial decomposition temperature of all the three copolymers (P(FHEMA-*co*-MAAT)s) was around 280 °C which could be due to the putrefaction of the azo group. Afterward, the second stage of weight loss appeared at around 365 °C which is ascribed to the decomposition of ester bonds (C=O and C–O) attached with the ferrocene. A large amount of carbon dioxide was released as a result which might be responsible for this weight loss. Lastly, Fe-C bonds were decomposed, forming a lot of Fe atoms which possibly catalyzed the degradation of polymers after 465 °C. Thermal stability of the copolymers might be increased due to the addition of azobenzene-based monomer which had the thermal

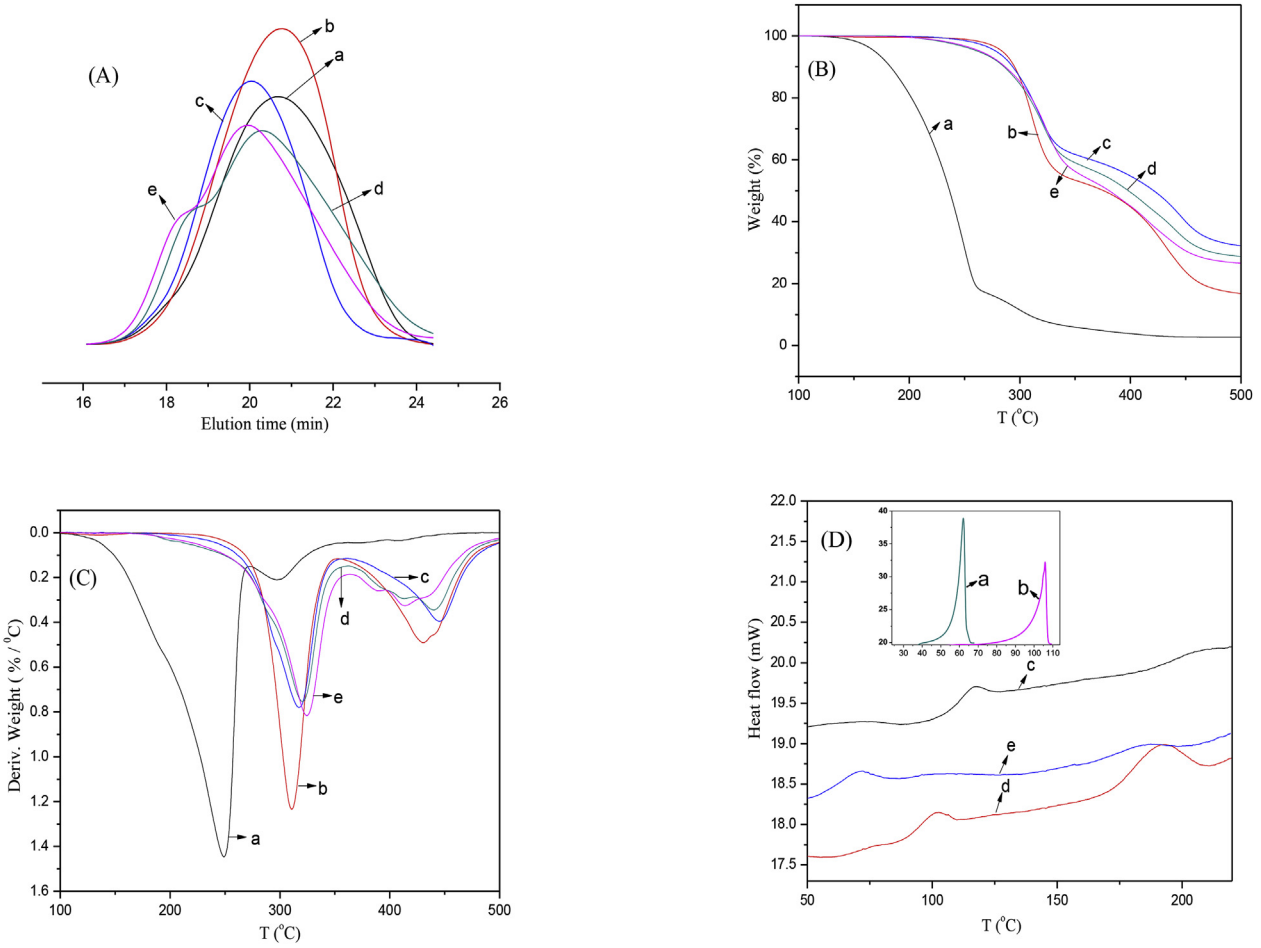

Fig. 3. (A) GPC curves of (a) PFHEMA, (b) PMAAT, (c) P(FHEMA-*co*-MAAT)-1, (d) P(FHEMA-*co*-MAAT)-2 and (e) P(FHEMA-*co*-MAAT)-3; (B) TGA curves of (a) PFHEMA, (b) PMAAT, (c) P(FHEMA-*co*-MAAT)-1, (d) P(FHEMA-*co*-MAAT)-2 and (e) P(FHEMA-*co*-MAAT)-3; (C) DTG curves of (a) PFHEMA, (b) PMAAT, (c) P(FHEMA-*co*-MAAT)-1, (d) P(FHEMA-*co*-MAAT)-2 and (e) P(FHEMA-*co*-MAAT)-3 and (D) DSC curves of (a) PFHEMA, (b) PMAAT, (c) P(FHEMA-*co*-MAAT)-1, (d) P(FHEMA-*co*-MAAT)-2 and (e) P(FHEMA-*co*-MAAT)-3.

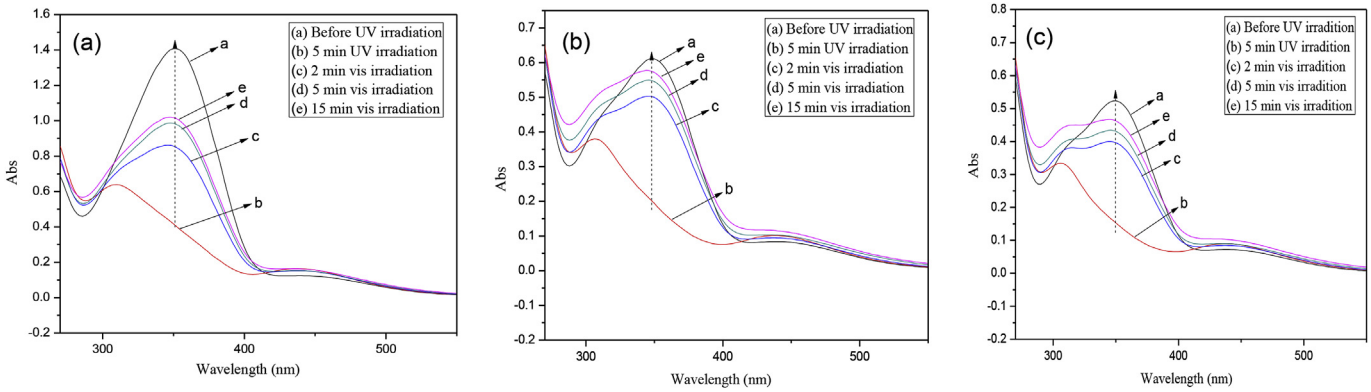

Fig. 4. Photo induced studies of (a) P(FHEMA-*co*-MAAT)-1, (b) P(FHEMA-*co*-MAAT)-2 and (c) P(FHEMA-*co*-MAAT)-3 at different time intervals.

stability up to 270 °C due to the high electron density and conjugate structure. The similar results could be observed in the case of DTG curves (Fig. 3C).

Fig. 3D shows the DSC curves of synthesized polymers whereas inset shows the melting temperature (T_m) of PFHEMA and PMAAT. The T_g of P(FHEMA-*co*-MAAT)-3 was found to be lower than those of the other two polymers. This might be due to the least percentage of an azo moiety in the polymer so its T_g became lower as compared to the other two polymers. The liquid crystalline phases can be observed from the DSC curves of P(FHEMA-*co*-MAAT)-2 and P(FHEMA-*co*-MAAT)-3. One possible explanation is that in these polymers the amount of mesogenic ferrocene unit is higher. This mesogenic ferrocene group imparted liquid crystalline properties to the polymer as explained by Amer and co-workers [25]. The azo group in the polymer enhances the size, rigidity and the polarity of the polymer chains. This enhancement usually results in the transition from the glass-like state to the rubber-like state at high temperatures.

3.4. Photo isomerization properties of P(FHEMA-co-MAAT)s

Photoinduced isomerization is considered as a backbone of azobenzene-containing polymers as this behavior can bring a lot of exciting applications such as optical data storage [26], molecular switches [27], display devices [28], nonlinear optical devices [29] and photochemical systems [30].

According to the conformational and isomerization behavior, azobenzenes have been classified into aminoazobenzene type, pseudo-stilbene type and azobenzene type molecules. Low (n-π*) and high (π-π*) absorption intensities can be observed depending

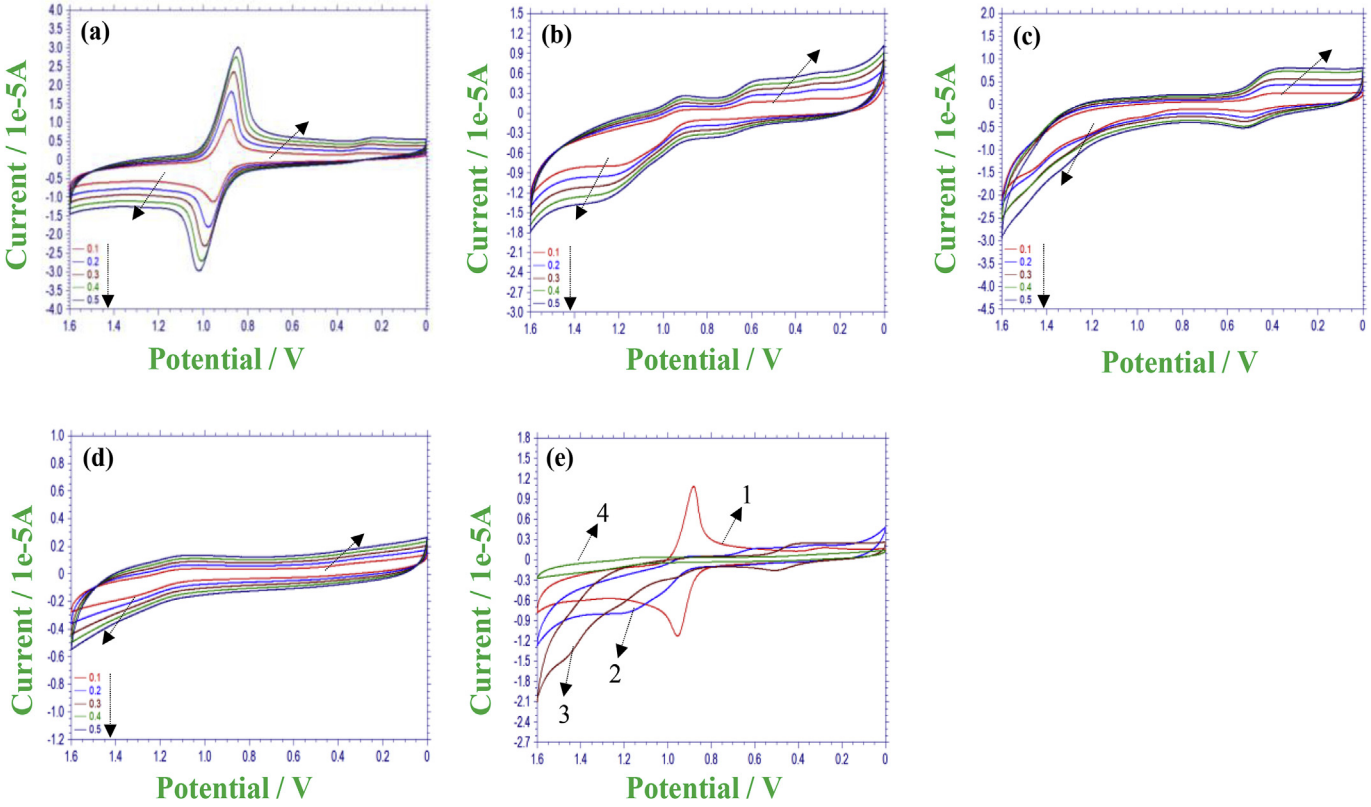

Fig. 5. CV curves of P(FHEMA-*co*-MAAT)-1 in (a) DCM, (b) DMF, (c) DMSO and (d) THF at different potential scan rates (direction of arrows means the increase of peaks in terms of current (oxidation and reduction) by increasing the scan rate) and (e) different organic solvents: (1) DCM, (2) DMF, (3) DMSO and (4) THF at 0.1 V/s.

on the type of source (UV/vis) for the azobenzene type of components. The UV-vis spectroscopy can be used easily for the monitoring of these type of molecules due to relatively slow *cis-trans* back relaxation [31]. To characterize the photoisomerization behavior of the polymers, the sample solutions were prepared in DMF.

The samples were irradiated using UV/vis light and their absorption spectra were recorded to capture the photoisomerization process of copolymers at different time intervals. The irradiation of UV light (364 nm) caused *trans* to *cis* isomerization which triggered a decrease in absorption intensity at around 390 nm from π-π* transition and an increase in absorption intensity at around 430 nm from n-π* transition. When the polymer solutions were exposed to visible light at different times, the reverse transition of azobenzene moiety can be observed as shown in Fig. 4(a–c). This spectral variation evidences that the synthesized polymers have photoisomerization behavior, showing an appealing application as light stimuli-responsive materials.

3.5. Electrochemical properties of P(FHEMA-co-MAAT)s

The electroactive polymers can give a lot of potential applications. Cyclic voltammetry is used extensively to explain and confirm the electro-responsive behavior of materials. The electrochemical behavior of the synthesized polymer can be affected by several factors such as scan rate, polarity/type of solvent and concentration of supporting electrolyte [32,33]. Therefore, it is expected that changing these influential parameters wisely can provide the optimum conditions that are important to find enhanced electrochemical properties.

Different solvents and scan rates affected the electrochemical properties of the synthesized polymers. The synthesized polymers showed different behavior by changing the parameters (scan rate and solvents). Organic solvents affected the shape of the CV curves due to the change in the polarity of the solvent. From Figs. 5–7, the shape of the curve was found to be more compact in case of DMSO and DMF due to their high polarity while the shape was more expanded in DCM and a little bit in THF because of their less polarity. Similarly, one redox peak was observed in the case of DCM whereas the solutions of THF, DMF and DMSO showed two or more than two redox peaks.

The reason behind obtaining two redox peaks might be related with the higher viscosity, less ion mobility and higher resistance of the solvents in comparison with DCM. The appearance of one redox peak showed that all the ferrocene units behaved equally whereas in high polar solvents the oxidized form of ferrocene was more stable and it was difficult to reduce. The similar behavior can be observed from the previously reported results by Wang et al. [33]. The synthesized polymers also showed sensitivity toward potential scan rate. It was found that the peak current values were increased by increasing the scan rate.

This increasing trend explained that the charge transport of the electrode evidenced Fick's law at room temperature. The rate of electrode reaction was faster in DCM in comparison with the other used solvents due to the smaller potential separation (peak to peak). The offered resistance by DCM was smaller and charge diffusion rate was faster than other solvents which explained the reason behind smooth occurring of redox reactions.

Similarly, the less steric hindrance between the synthesized copolymers eased the electron transport characteristics which showed distinct oxidation and reduction peaks in CV studies. These results indicated that reversible electrochemical processes can be achieved by using these synthesized polymers in this work. It was found that the synthesized copolymers in this work can be used for the storage of optical and electrical information. For the better

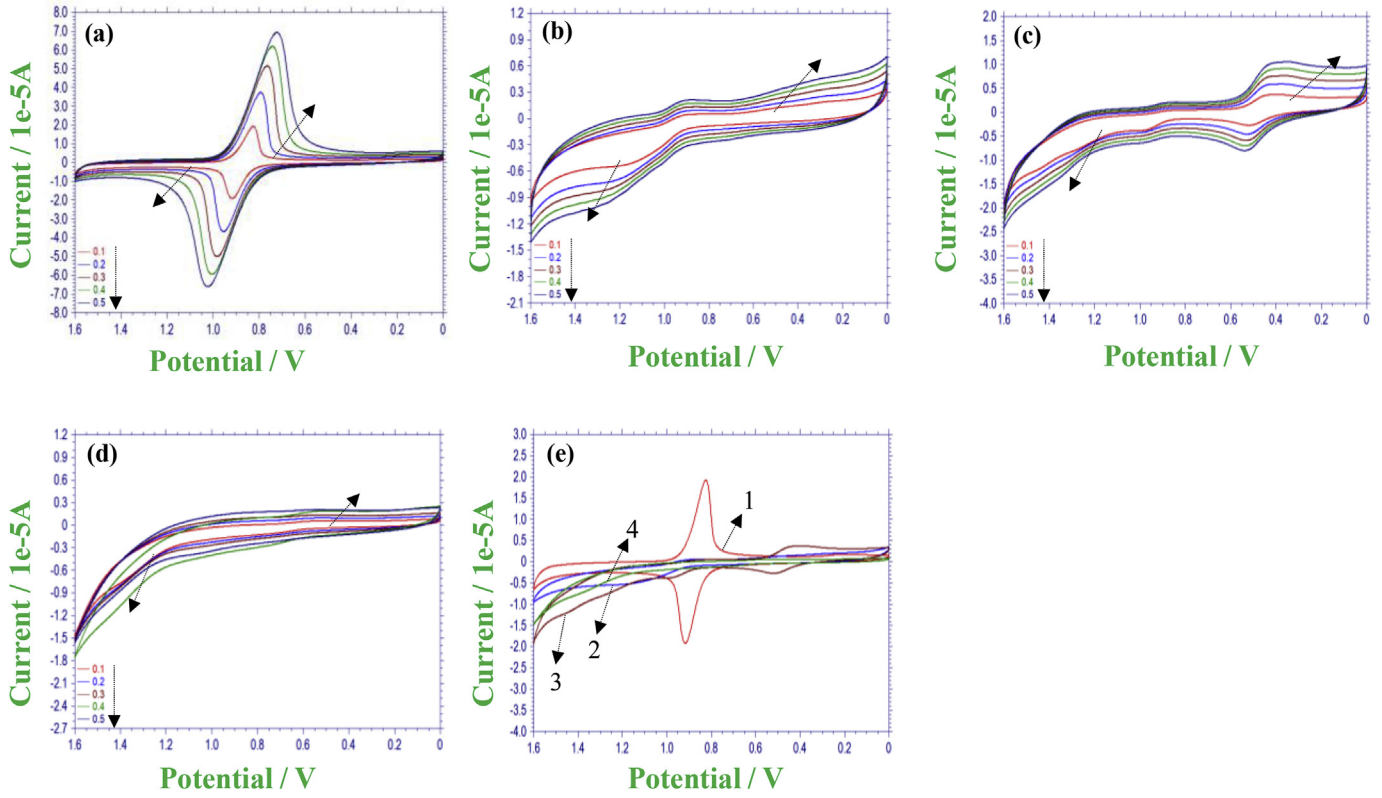

Fig. 6. CV curves of P(FHEMA-*co*-MAAT)-2 in (a) DCM, (b) DMF, (c) DMSO and (d) THF at different potential scan rates (direction of arrows means the increase of peaks in terms of current (oxidation and reduction) by increasing the scan rate) and (e) different organic solvents: (1) DCM, (2) DMF, (3) DMSO and (4) THF at 0.1 V/s.

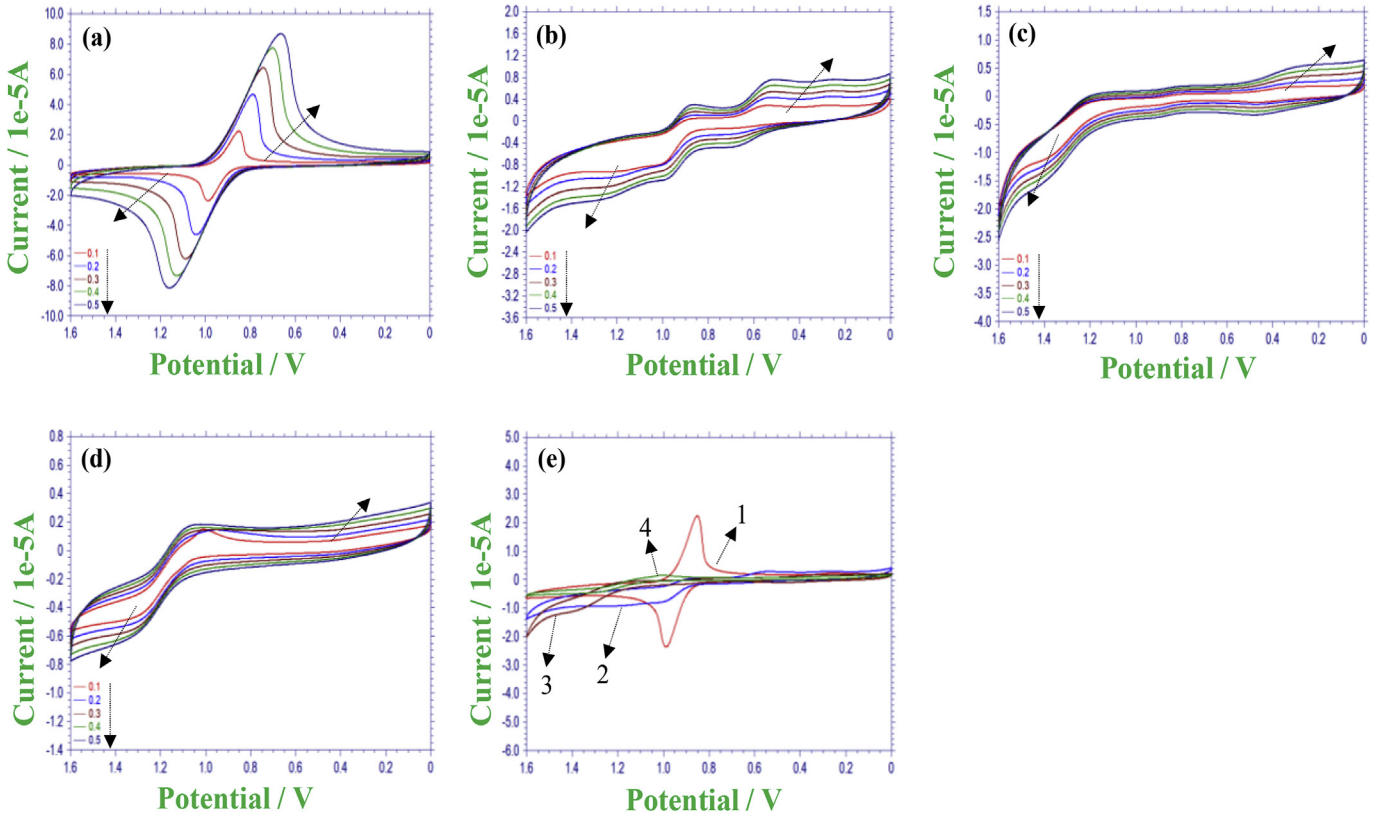

Fig. 7. CV curves of P(FHEMA-*co*-MAAT)-3 in (a) DCM, (b) DMF, (c) DMSO and (d) THF at different potential scan rates (direction of arrows means the increase of peaks in terms of current (oxidation and reduction) by increasing the scan rate) and (e) different organic solvents: (1) DCM, (2) DMF, (3) DMSO and (4) THF at 0.1 V/s.

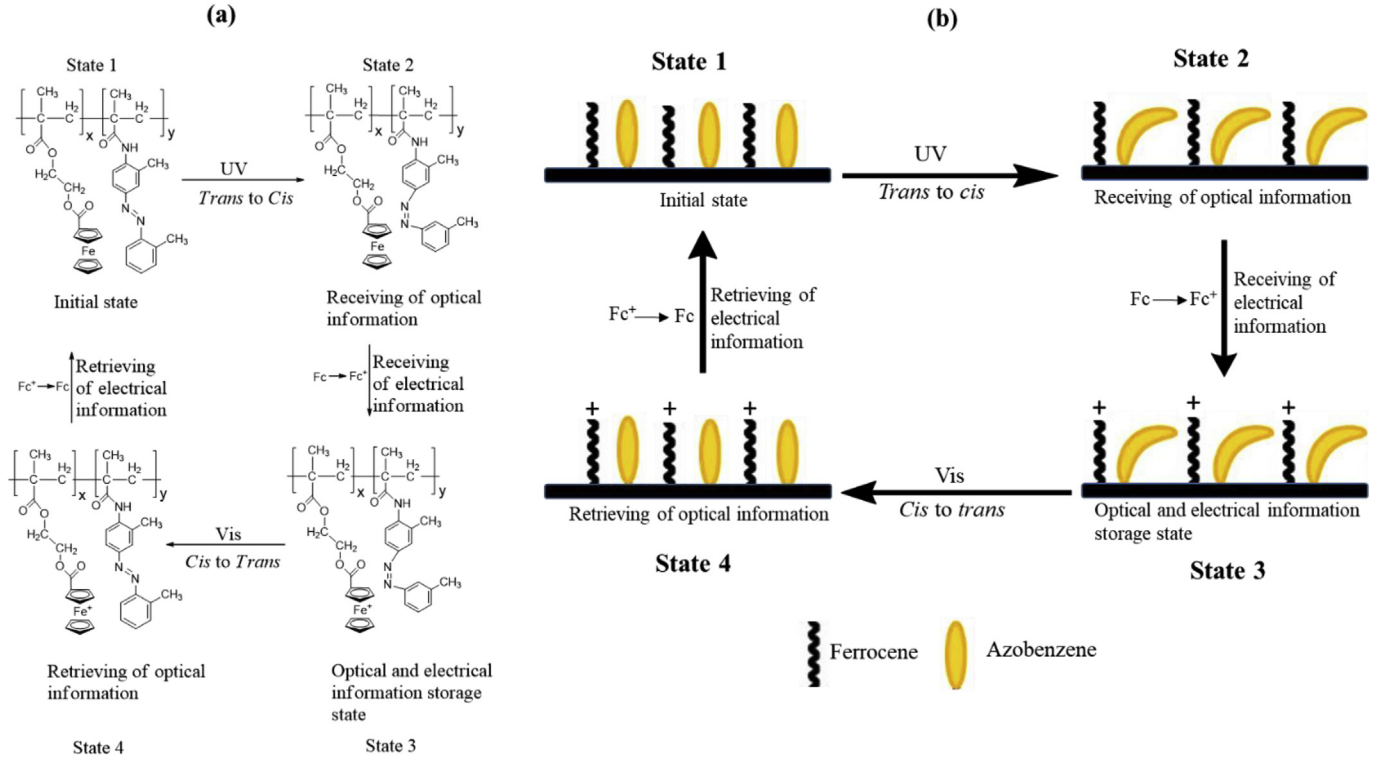

Fig. 8. (a) Possible schematic view representing the information storage application and (b) pictorial view of the information storage application based on polymers containing ferrocene and azobenzene.

understanding, schematic and pictorial views have been shown in Fig. 8.

In the first step, UV light incidents and *trans* azobenzene changes to *cis* azobenzene which can be regarded as state 2 (optical information storage stage). In the third state, electrical information is stored, when ferrocene changes to ferrocenium ion (Fc to Fc^{+}). The fourth state corresponds with *cis* to *trans* isomerization of azobenzene after consuming visible light and at the end ferrocenium ion turns into its initial state after retrieving the electrical information (electrochemical stimulus).

4. Conclusion

In this study, we focused on the stimuli-responsive behavior of ferrocene and azobenzene. For this purpose, three different copolymers named as P(FHEMA-*co*-MAAT)-1, P(FHEMA-*co*-MAAT)-2 and P(FHEMA-*co*-MAAT)-3 were synthesized using free radical polymerization and characterized by ^{1}H NMR spectra. Thermal stability of the polymers was confirmed using TG/DTG analysis. These resulting copolymers showed excellent redox and photo-responsive properties which were confirmed with the help of cyclic voltammetry and UV/vis spectroscopy. It was concluded that when these moieties were combined together, they showed very useful electro-photo responsive behavior which can be further used for information storage application.

Acknowledgment

Financial support from the National Natural Science Foundation of China (51673170, 21472168, 21372200 and 21611530689), the Science and Technology Innovation Team of Ningbo (2011B82002), the Fundamental Research Funds for the Central Universities (2017FZA4023) are gratefully acknowledged.

Appendix A. Supplementary data

Supplementary data to this article can be found online at https://doi.org/10.1016/j.jorganchem.2018.10.033.

References

[1] X. Xia, H. Yu, L. Wang, Z. Deng, K.J. Shea, Zain-ul-Abdin, Eur. Polym. J. 100 (2018) 103–110.
[2] S. Kaur, M. Kaur, P. Kaur, K. Clays, K. Singh, Coord. Chem. Rev. 343 (2017) 185–219.
[3] T. Morikita, T. Yamamoto, J. Organomet. Chem. 637 (2001) 809–812.
[4] K. Fujiwara, H. Akutsu, J.I. Yamada, M. Satoh, S.I. Nakatsuji, Tetrahedron Lett. 52 (2011) 6655–6658.
[5] R. Hudson, J. Organomet. Chem. 637 (2001) 47–69.
[6] S. Wang, Z. Xu, T. Wang, T. Xiao, X.Y. Hu, Y.-Z. Shen, L. Wang, Nat. Commun. 9 (2018) 1–7.
[7] O. Bertrand, J.-F. Gohy, Polym. Chem. 8 (2017) 52–73.
[8] E.R. Ruskowitz, C.A. DeForest, Nat. Rev. Mater. 3 (2018) 17087–17104.
[9] A. Kozanecka-Szmigiel, J. Antonowicz, D. Szmigiel, M. Makowski, A. Siemion, J. Konieczkowska, B. Trzebicka, E. Schab-Balcerzak, Polymer 140 (2018) 117–121.
[10] V.V. Jerca, R. Hoogenboom, Angew. Chem. Int. Ed. 57 (2018) 7945–7947.
[11] M. Abboud, R. Bel-Hadj-Tahar, N. Fakhri, A. Sayari, Microporous Mesoporous Mater. 265 (2018) 179–184.
[12] R. Zhang, Y.J. Ji, L. Yang, Y. Zhang, G.C. Kuang, Phys. Chem. Chem. Phys. 18 (2016) 9914–9917.
[13] G.S. Kumar, D. Neckers, Chem. Rev. 89 (1989) 1915–1925.
[14] A. Samanta, D.B.J. Ravoo, Chem. Eur J. 20 (2014) 4966–4973.
[15] M. Kurihara, A. Hirooka, S. Kume, M. Sugimoto, H. Nishihara, J. Am. Chem. Soc. 124 (2002) 8800–8801.
[16] T. Asano, T. Okada, Chem. Inf. 16 (1985) 4387–4391.
[17] M.R. Molla, P. Rangadurai, L. Antony, S. Swaminathan, J.J. de Pablo, S. Thayumanavan, Nat. Chem. 10 (2018) 659–666.
[18] V. Malatesta, M. Milosa, R. Millini, L. Lanzini, P. Bortolus, S. Monti, Mol. Cryst. Liq. Cryst. 246 (2006) 303–310.
[19] P. Weis, D. Wang, S. Wu, Macromolecules 49 (2016) 6368–6373.
[20] Z. Wang, H. Tian, K. Chen, Dyes Pigments 51 (2001) 161–165.
[21] H. Yu, L. Wang, H. Jia, J. Ding, Q. Tan, J. Appl. Polym. Sci. 110 (2010) 1594–1599.
[22] M. Saleem, L. Wang, H. Yu, Zain-ul-Abdin, M. Akram, R.S. Ullah, Colloid Polym. Sci. 295 (2017) 995–1006.
[23] Y. Sun, N. Zhou, W. Zhang, Y. Li, Z. Cheng, J. Zhu, Z. Zhang, X. Zhu, J. Polym. Sci. Part A Polymer Chemistry 50 (2012) 3788–3796.
[24] C. Yuan, J. Guo, M. Tan, M. Guo, L. Qiu, F. Yan, ACS Macro Lett. 3 (2014) 271–275.
[25] W.A. Amer, L. Wang, A.M. Amin, H. Yu, L. Zhang, C. Li, Y. Wang, Polym. Adv. Technol. 24 (2013) 181–190.
[26] T. Gao, Y. Xue, Z. Zhang, W. Que, Optic Express 26 (2018) 4309–4317.
[27] S. Jaekel, A. Richter, R. Lindner, R. Bechstein, C. Nacci, S. Hecht, A. Kühnle, L. Grill, ACS Nano 12 (2018) 1821–1828.
[28] K. Goda, M. Omori, K. Takatoh, Liq. Cryst. 45 (2018) 485–490.
[29] B. Kulyk, D. Guichaoua, A. Ayadi, A. El-Ghayoury, B. Sahraoui, Dyes Pigments 145 (2017) 256–262.
[30] L.Q. Zheng, X. Wang, F. Shao, D.M. Hegner, D.R. Zenobi, Angew. Chem. Int. Ed. 129 (2017) 1–6.
[31] Y. Zhao, J. He, Soft Matter 5 (2009) 2686–2693.
[32] H.J. Yu, L. Wang, J. Huo, C. Li, Q. Tan, Des. Monomers Polym. 12 (2009) 305–313.
[33] X.J. Wang, L. Wang, J.J. Wang, T. Chen, Electrochim. Acta 52 (2007) 3941–3949.